



Since January 2020 Elsevier has created a COVID-19 resource centre with free information in English and Mandarin on the novel coronavirus COVID-19. The COVID-19 resource centre is hosted on Elsevier Connect, the company's public news and information website.

Elsevier hereby grants permission to make all its COVID-19-related research that is available on the COVID-19 resource centre - including this research content - immediately available in PubMed Central and other publicly funded repositories, such as the WHO COVID database with rights for unrestricted research re-use and analyses in any form or by any means with acknowledgement of the original source. These permissions are granted for free by Elsevier for as long as the COVID-19 resource centre remains active.



Available online at [www.sciencedirect.com](http://www.sciencedirect.com)

ScienceDirect

journal homepage: [www.e-jmii.com](http://www.e-jmii.com)



ORIGINAL ARTICLE

# Phage display technique identifies the interaction of severe acute respiratory syndrome coronavirus open reading frame 6 protein with nuclear pore complex interacting protein NPIP3 in modulating Type I interferon antagonism



Su-Hua Huang<sup>a</sup>, Tzu-Ying Lee<sup>b</sup>, Ying-Ju Lin<sup>c</sup>, Lei Wan<sup>c</sup>,  
Chih-Ho Lai<sup>d</sup>, Cheng-Wen Lin<sup>a,b,\*</sup>

<sup>a</sup> Department of Biotechnology, Asia University, Wufeng, Taichung, Taiwan

<sup>b</sup> Department of Medical Laboratory Science and Biotechnology, China Medical University, Taichung, Taiwan

<sup>c</sup> Department of Medical Genetics and Medical Research, China Medical University Hospital, Taichung, Taiwan

<sup>d</sup> School of Medicine, Department of Microbiology, China Medical University, Taichung, Taiwan

Received 27 January 2015; received in revised form 9 June 2015; accepted 6 July 2015

Available online 31 July 2015

## KEYWORDS

IFN antagonism;  
NPIP3;  
ORF6;  
phage display;  
SARS-CoV

**Abstract** *Background/Purpose:* Severe acute respiratory syndrome coronavirus (SARS-CoV) proteins including ORF6 inhibit Type I interferon (IFN) signaling.

*Methods:* This study identified SARS-CoV ORF6-interacting proteins using the phage displayed human lung cDNA libraries, and examined the association of ORF6–host factor interaction with Type I IFN antagonism. After the fifth round of biopanning with *Escherichia coli*-synthesized ORF6-His tagged protein, the relative binding affinity of phage clones to ORF6 was determined using direct enzyme-linked immunosorbent assay.

*Results:* The highest affinity clone to ORF6 displayed the C-terminal domain of NPIP3 (nuclear pore complex interacting protein family, member B3; also named as phosphatidylinositol-3-kinase-related kinase SMG-1 isoform 1 homolog). The coimmunoprecipitation assay demonstrated the direct binding of ORF6 to the C-terminal domain of NPIP3 *in vitro*. Confocal

\* Corresponding author. Department of Medical Laboratory Science and Biotechnology, China Medical University, Number 91, Hsueh-Shih Road, Taichung 40402, Taiwan.

E-mail address: [cwlin@mail.cmu.edu.tw](mailto:cwlin@mail.cmu.edu.tw) (C.-W. Lin).

imaging revealed a close colocalization of SARS-CoV ORF6 protein with NPIP3 in human promonocytes. The dual luciferase reporter assay showed that the C-terminal domain of NPIP3 attenuated the antagonistic activity of SARS-CoV ORF6 on IFN- $\beta$ -induced ISRE (IFN stimulated response element)-responsive firefly luciferase activity. In addition, confocal imaging and Western blotting assays revealed that the increases in STAT-1 nuclear translocation and phosphorylation occurred in the transfected cells expressing both genes of ORF6 and NPIP3, but not in the ORF6-expressing cells in response to IFN- $\beta$ .

**Conclusion:** The overexpression of NPIP3 restored the IFN- $\beta$  responses in SARS-CoV ORF6 expressing cells, indicating that the interaction of SARS CoV ORF6 and NPIP3 reduced Type I IFN antagonism by SARS-CoV ORF6.

Copyright © 2015, Taiwan Society of Microbiology. Published by Elsevier Taiwan LLC. This is an open access article under the CC BY-NC-ND license (<http://creativecommons.org/licenses/by-nc-nd/4.0/>).

## Introduction

The pandemic outbreak of severe acute respiratory syndrome coronavirus (SARS-CoV) arose from Guangdong Province of China in November 2002, and eventually infected > 8500 people worldwide.<sup>1,2</sup> The Middle East respiratory syndrome coronavirus (MERS-CoV), which emerged from the Arabian Peninsula in 2012, was globally identified in 941 laboratory-confirmed cases with 347 related deaths until December 26, 2014, according to the World Health Organization (<http://www.who.int/csr/don/26-december-2014-mers/en/>). The CoV genome is a single-stranded, positive-sense RNA of ~30 kb; it contains 14 potential open reading frames (ORFs) and encodes replicase (ORF1a and ORF1ab), structural proteins (spike, nucleocapsid, membrane, and envelope), and accessory proteins (ORF 3a, ORF 3b, ORF6, ORF 7a, ORF 7b, ORF 8a, ORF 8b, and ORF 9b).<sup>3</sup> These accessory proteins could be dispensable for virus replication, but might have a specific function in viral infection. ORF3 and ORF 7a proteins activate JNK (c-Jun N-terminal kinase) and NF- $\kappa$ B (nuclear factor kappa B) signaling, upregulate interleukin-8 and RANTES (regulated on activation, normal T expressed and secreted), and modulate apoptosis and cell cycle.<sup>4,5</sup> ORF 3b and ORF6 proteins modulate the host innate immune response, including inhibition of Type I IFN production and signaling.<sup>4,5</sup>

The SARS-CoV ORF6 protein localizes in the membrane of endoplasmic reticulum (ER) and Golgi apparatus in infected cells<sup>6</sup>; ORF6 overexpression triggers the ER stress in transfected cells.<sup>7</sup> The ORF6 protein is dispensable for viral replication *in vitro* and *in vivo*,<sup>8</sup> but associates with viral escape from the innate immune system, particularly inhibition of Type I interferon (IFN) production and signaling pathways.<sup>7,9</sup> ORF6 protein interacts with the C terminus of karyopherin alpha 2, leading to impeding the nuclear import of phosphorylated signal transducer and activator of transcription 1 (STAT1) in response to IFN- $\beta$ . Thus, SARS-CoV ORF6 protein is an antagonist of Type I IFNs. In this study, we identified cellular ORF6-interacting factors using phage display human lung cDNA library, further examining the association of SARS-CoV ORF6 and host factors in Type I IFN antagonism. The C terminus of nuclear pore complex interacting protein NPIP3 (nuclear

pore complex interacting protein family, member B3; Gene ID: 23117), also known as phosphatidylinositol (PI)-3-kinase-related kinase SMG-1 isoform 1 homolog, displayed on phage surface showed the highest binding affinity to recombinant ORF6 protein. The interaction of ORF6 and NPIP3 was analyzed using coimmunoprecipitation *in vitro* and colocalization in cells. The effect of NPIP3 overexpression on Type I IFN antagonism of ORF6 was determined using dual-luciferase reporter assay system, and STAT1 phosphorylation and nuclear translocation.

## Methods

### Construction and expression of recombinant ORF6 protein in *Escherichia coli* and human promocyte HL-CZ cells

For generating bacterial and mammalian expression of recombinant ORF6 protein, the SARS-CoV ORF6 gene of the SARS-CoV TW1 strain genome (GenBank Accession No. AY291451) was amplified by reverse transcription-polymerase chain reaction (RT-PCR) from genome RNA template and cloned into the pTriE-4 Neo vector for the production of the recombinant ORF6 protein fused with an N-terminal His-tag. The primers included 5'-ATCGGAATTC-TATGTTTCATCCGTT-3' and 5'-ATCGGCGGCCGCTGGATAAT-CTAACTC-3'. The forward primer contained an *Eco*RI restriction site; the reverse primer included a *Not*I restriction site. The amplified RT-PCR product was cloned into the pTriEx-4 Neo vector (Novagen, Madison, Wisconsin, USA), resulting in construct named pTriEx-ORF6. For the production of *E. coli*-synthesized ORF6 protein, pTriEx-ORF6 was transformed into *E. coli* BL21 (DE3) cells. The induction expression and purification of *E. coli*-synthesized ORF6 protein were performed as described in our prior reports.<sup>10,11</sup> Finally, the recombinant ORF6 protein was purified using immobilized-metal affinity chromatography as described in our previous study,<sup>12</sup> and then analyzed by Western blotting with anti-His-tag monoclonal antibody and alkaline phosphatase-conjugated goat antimouse immunoglobulin G (IgG) antibodies. The immunoreactive band was developed with tetranitroblue tetrazolium/5-bromo-4-

chloro-3- idolyphosphate (TNBT/BCIP) (Gibco, Invitrogen, Merelbeke, Belgium) (Invitrogen).

### Biopanning of a phage display human cDNA library with SARS-CoV ORF6 protein

For identifying ORF6-interacting proteins, a human lung cDNA library (Novagen, Madison, Wisconsin, USA) was used to screen high-affinity phage clones to recombinant ORF6, as previously described.<sup>10,11</sup> Briefly, biopanning of the phage display lung cDNA library was performed using ORF6-coated microplates. After five rounds of biopanning, ORF6-interacting phage clones were eluted with the soluble ORF6 protein. The ORF6-interacting phage clone was randomly picked up from individual plaques, amplified in *E. coli*, and then used for determining the binding affinity to the recombinant ORF6 protein using direct enzyme-linked immunosorbent assay. The nucleotide sequences of ORF6-interacting proteins displayed on the high-affinity phage clones were directly sequenced; their deduced amino acid sequences were analyzed using BLAST search (<http://www.ncbi.nlm.nih.gov/BLAST/>).

### Coimmunoprecipitation and colocalization assays

The nucleotide sequences of the C terminus (amino acid residues 936–1050) of NPIP3 (Accession Number Q92617) fused with the coat protein of ORF6-interacting phage clone 40 was amplified using PCR, and then cloned into bacterial expression vector pET32a for coimmunoprecipitation *in vitro* and mammalian expression vector pDsRed1-C (BD Biosciences Clontech) for colocalization assay. The two primer pairs were 5'-ATCGGATATCTCAAGCGAGGCAGAAAAA-3' and 5'-ATCGGAATTCGCTCAACCTCCGCCTCTT-3' for pET32a cloning, as well as 5'- ATCGATGAAGCTTATTCAAGCGAGGCA-GAA-3' and 5'-ATCGATGGGATCCGCTCAA-CCTCCGCCTCTT-3' for pDsRed1-C cloning, respectively. For coimmunoprecipitation assays, *E. coli* BL21 (DE3) cells were transformed with pET32a-NPIP3; the *E. coli*-synthesized C-terminal domain of NPIP3 protein was induced and purified using immobilized-metal affinity chromatography as described in our prior studies.<sup>10–12</sup> The recombinant C-terminal domain of NPIP3 with a thioredoxin (Trx) at the N terminus and a His-tag at the C terminus was mixed with the recombinant ORF6 protein with an N-terminal His-Tag; the mixture was incubated with the anti-Trx mAb overnight in a cool room, followed by addition of protein A-Sepharose beads for an additional 2 hours. After centrifugation (16,000 × g, 15 minutes), the immunoprecipitate was analyzed using Western blotting with the anti-His tag mAb for a 1-hour incubation period. The immune-reactive complexes were detected using horseradish peroxidase-conjugated goat antimouse IgG antibodies, and then developed using enhanced chemiluminescence reaction (Amersham Pharmacia Biotech). For colocalization assays, pTriEx-ORF6 plus pDsRed1-C (BD Biosciences Clontech), pTriEx-ORF6 plus pDsRed-NPIP3, pTriEx plus pDsRed1-C, or pTriEx plus pDsRed-NPIP3 were cotransfected into HL-CZ cells (human promonocyte cell line) with GenePorter cells. Transfected cells were generated, fixed, and stained with primary antibodies against His-tag, followed by fluorescein isothiocyanate

(FITC)-conjugated antimouse IgG antibodies, as described in our previous studies.<sup>13,14</sup> A confocal image of stained cells was taken using Leica TCS SP2 AOBs laser scanning microscopy (Leica Microsystems, Heidelberg GmbH, Germany). In cells, red fluorescence indicated DsRed-NPIP3 fusion protein, whereas green fluorescence was ORF6-His tag fusion protein. The colocalization of DsRed-NPIP3 and ORF6 appeared orange to yellow in color.

### Dual-luciferase reporter assay of IFN stimulated response element promoter

HL-CZ cells expressing single and both of ORF6 and NPIP3, described above, were further cotransfected with pISRE-Luc *cis*-reporter (Stratagene) and control reporter pRluc-C1, treated with IFN- $\beta$  (Hoffmann-La Roche) for 4 hours, and then harvested. The activity of experimental firefly luciferase and control renilla luciferase in lysate was measured using dual Luciferase Reporter Assay System (Promega) and TROPIX TR-717 Luminometer (Applied Biosystems) described by Lin et al.<sup>11</sup>

### Subcellular localization assays of STAT1

HL-CZ cells expressing single and both of ORF6 and NPIP3, described above, were treated with IFN- $\beta$  (Hoffmann-La Roche) for 1 hour, and then harvested. Cells were fixed by cold methanol, incubated with anti-STAT1 mAb for 2 hours, followed by FITC-conjugated antimouse IgG antibodies for additional 2 hours. Finally, cells were stained with 4',6-diamidino-2-phenylindole for 10 minutes. Photographs of cells were taken using immunofluorescent microscopy.

### Western blotting of STAT1 phosphorylation

For testing the effect of ORF6 and NPIP3 interaction on IFN-stimulated STAT1 activation, lysate from cells expressing single and both of ORF6 and NPIP3 treated with IFN- $\beta$  for 15 minutes and 30 minutes was obtained using Western blotting with antiphosphotyrosine STAT1 (Tyr701), and anti- $\beta$  actin mAb (Cell Signaling Technology). The immune-reactive bands were probed using horseradish peroxidase-conjugated goat antimouse IgG antibodies, and then developed using enhanced chemiluminescence reagents.

### Statistical analysis

Three independent experiments in each independent result were performed; all data are represented as mean  $\pm$  standard deviation and statistically analyzed using SPSS software (version 10.1; SPSS Inc., Chicago, IL, USA) via one-way analysis of variance analysis by Scheffe's test.

## Results

### Selection of SARS-CoV ORF6-interacting host factors using phage display library

SARS-CoV ORF6, cloned into the pTriEx-4 vector, was synthesized as a 17.5-kDa fusion protein with an N-terminal

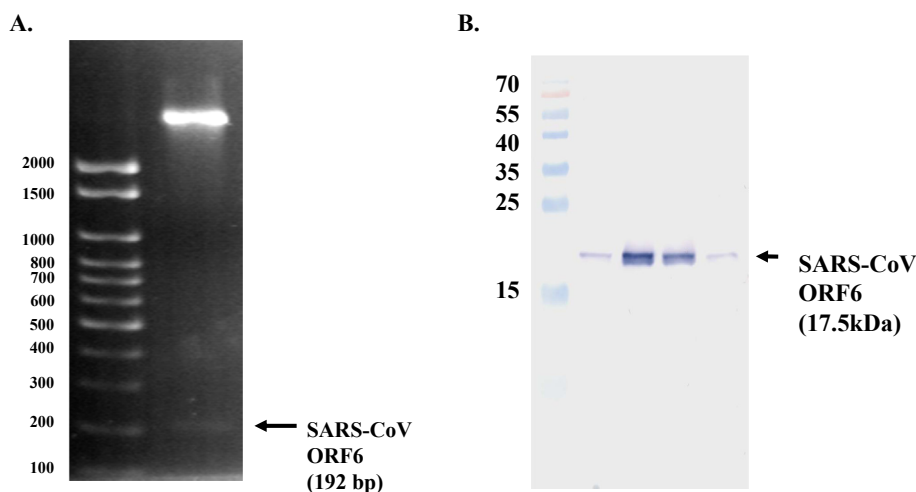


**Figure 1.** Expression and purification of *Escherichia coli*-synthesized SARS-CoV ORF6 protein. The ORF6 gene was amplified using PCR and cloned into pTriEx-4 Neo vector (A). ORF6-His tagged proteins were synthesized in transformed *E. coli* BL21 (DE3), purified using immobilized-metal affinity chromatography, separated using SDS-PAGE, and then examined using Western blotting with anti-His tag (B). ORF = open reading frame; PCR = polymerase chain reaction; SARS-CoV = severe acute respiratory syndrome coronavirus; SDS-PAGE = sodium dodecyl sulfate-polyacrylamide gel electrophoresis.

His-Tag in *E. coli* that was purified using immobilized-metal affinity chromatography (Figure 1). The recombinant ORF6 protein was used for the selection of its interacting cellular factors with phage-displayed human lung cDNA library. After the fifth round of biopanning, ORF6-specific binding phage clones eluted were selected from single phage plaques, amplified in *E. coli* for determining relative ORF6-

binding affinities. Each phage clone was performed by direct binding enzyme-linked immunosorbent assay in ORF6-coated wells (Figure 2). Phage clone numbers 16, 26, and 40 with higher binding affinity to ORF6 were quantitated using plaque assays ( $p < 0.01$ ), and we subsequently measured the binding specificity (Figure 3). Phage clones numbers. 16, 26, and 40 bound to the recombinant ORF6 protein in a

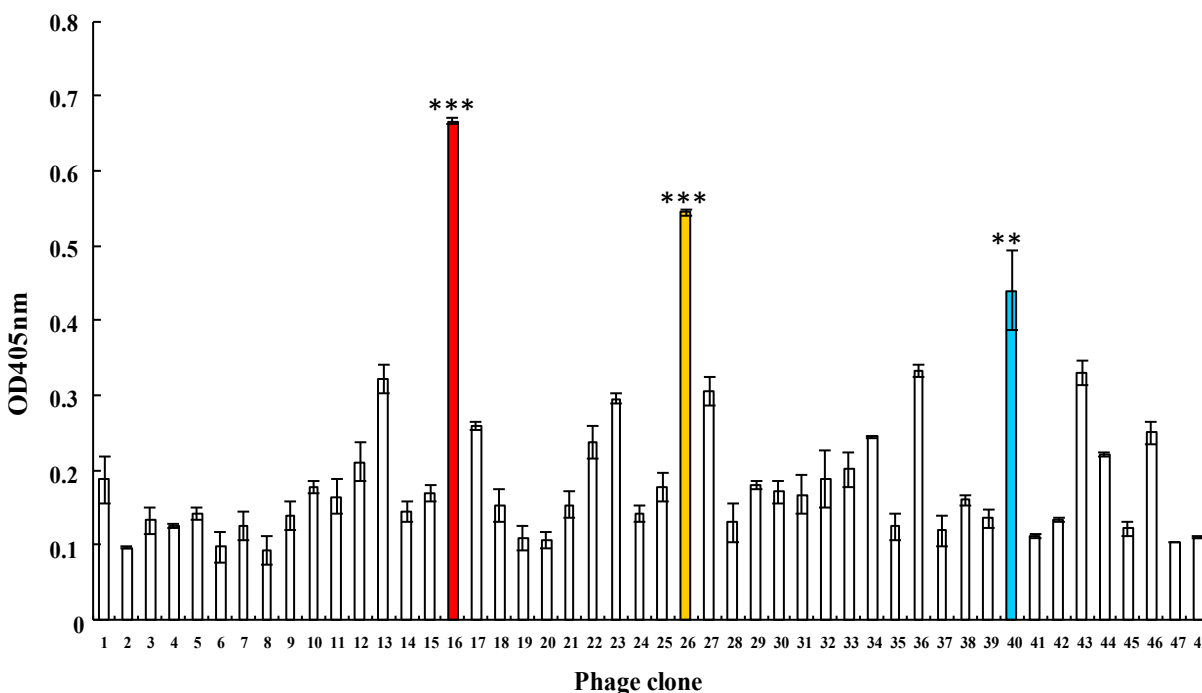


**Figure 2.** Biopanning of phage display a human lung cDNA library with ORF6-His tagged protein. After the fifth round of biopanning with ORF6, each phage clone was randomly picked up from individual plaques, amplified in *Escherichia coli*, and performed using direct binding ELISA with ORF6-coated plates and antiphage antibodies. \*  $p < 0.05$ , by Scheffe's test. \*\*  $p < 0.01$ , by Scheffe's test. \*\*\*  $p < 0.001$ , by Scheffe's test. ELISA = enzyme-linked immunosorbent assay; ORF = open reading frame.

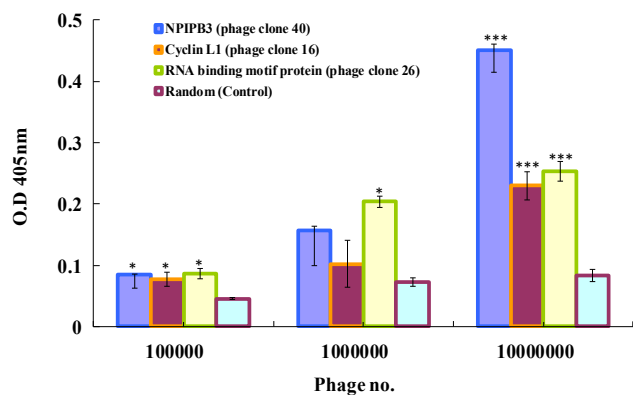


**Figure 3.** Direct binding ELISA of high-affinity phage clones to ORF6-His tagged protein. High-affinity phage clone was amplified in *Escherichia coli*, quantitated using plaque assay, and then performed by direct binding ELISA with ORF6-coated plates and antiphage antibodies. \*  $p < 0.05$ , by Scheffe's test. \*\*  $p < 0.01$ , by Scheffe's test. \*\*\*  $p < 0.001$ , by Scheffe's test. ELISA = enzyme-linked immunosorbent assay; ORF = open reading frame.

dose-dependent manner. Among the three phage clones, clone number 40 at a titer of  $10^7$  phages showed the highest affinity to ORF6 protein ( $p < 0.001$ ). ORF6-interacting protein-encoding sequences fused in-frame with protein III gene of phage clone numbers 16, 26, and 40 were sequenced. A BLAST alignment search of the nucleotide sequences indicated that ORF6-interacting protein display phage clone numbers 16, 26, and 40 were identified as CCN1 (cyclin L1), RBML2 (RNA binding motif protein, X-linked-like 2), and NPIP3 (nuclear pore complex interacting protein family, member B3), respectively. Because NPIP3 displayed on phage clone 40 had the highest binding affinity to ORF6 protein (Figure 3), the interaction between ORF6 and NPIP3 was further evaluated.

### *In vitro* and *in vivo* interaction of ORF6 with NPIP3

To test *in vitro* and *in vivo* interaction between ORF6 and NPIP3, the C terminus (amino acid residues 936–1050) of NPIP3 was cloned into bacterial expression vector pET32a for *in vitro* coimmunoprecipitation and mammalian expression vector pDsRed1-C for *in vivo* colocalization assay (Figures 4 and 5). In the coimmunoprecipitation assay, the ORF6-His tag protein reacted with the Trx-NPIP3-His tag fusion protein for 4 hours in a cool room, and then the protein complex were coimmunoprecipitated using anti-Trx antibodies and protein A-Sepharose beads. The coimmunoprecipitates were analyzed using Western blotting with the anti-His tag antibodies (Figure 4). The Western blotting analysis of immunoprecipitates revealed that the ORF6 protein bound to the Trx-NPIP3-His tag fusion protein, but not to Trx protein (Figure 4, lane 3 vs. lane 1). In the colocalization assay, single and both of DsRed-NPIP3 and ORF6-His tag proteins were expressed in human promonocyte HL-CZ cells. After immunofluorescence staining with anti-His tag and FITC-conjugated antimouse IgG antibodies, confocal microscopy revealed a very close colocalization of

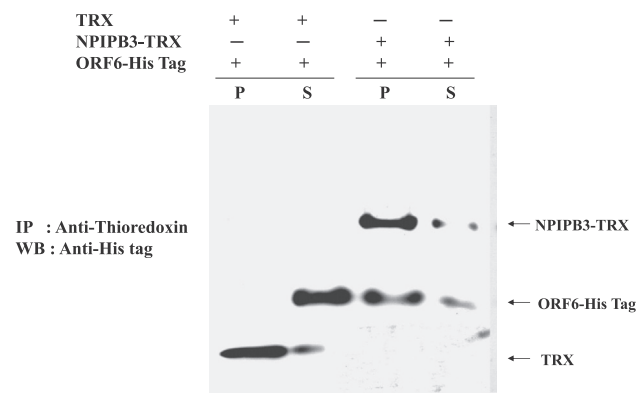


**Figure 4.** Coimmunoprecipitation of ORF6-His tagged protein with Trx-NPIP3 fusion protein. Purified ORF6-His tagged protein mixed with Trx-NPIP3 fusion protein was incubated with anti-Trx antibodies at 4°C overnight, followed by incubation with protein A-Sepharose beads for a further 2 hours. After centrifugation, the pellet was washed with NET buffer, samples were analyzed by SDS-PAGE, Western blotting, and immunoanalysis using rabbit anti-Trx and mouse anti-His tag antibodies. NPIP3 = nuclear pore complex interacting protein family, member B3; ORF = open reading frame; SDS-PAGE = sodium dodecyl sulfate-polyacrylamide gel electrophoresis; Trx = thioredoxin.

DsRed-NPIP3 and ORF6-His tag protein appearing as orange to yellow fluorescent light (Figure 5P), but no colocalization between DsRed and ORF6-His tag protein, or DsRed-NPIP3 and His tag protein (Figures 5D, 5H, and 5L). The results demonstrated SARS-CoV ORF6 directly interacting with the C terminus of NPIP3 *in vitro* and *in vivo*.

### Attenuation effect of NPIP3 overexpression on Type I IFN antagonistic activity of SARS-CoV ORF6

To determine the role of NPIP3 in Type I IFN antagonism of SRAS-CoV ORF6, the IFN- $\beta$  induced responses of transfected cells with single or both of pDsRed-NPIP3 and pTriEx-ORF6 were explored using ISRE (IFN stimulated response element) luciferase reporter, STAT1 subcellular localization, and Western blotting assays (Figures 6–8). Transient overexpression of NPIP3 C terminus improved with 2.5-fold increase of the ISRE promoter activity in ORF6-expressing cells in response to IFN- $\beta$  (Figure 6;  $p < 0.001$ ). To examine the subcellular location of STAT1, confocal imaging analysis indicated that the overexpression of NPIP3 C terminus did not change the subcellular localization of STAT1 in vector control and ORF6-expressing cells [Figure 7A(4)–(6) and 7A(10)–(12)]. The IFN- $\beta$  treatment stimulated STAT1 nuclear translocation in vector control cells [Figures 7B(1)–(3)], but not in ORF6-expressing cells [Figure 7B(7)–(9)]. However, NPIP3 C terminus overexpression significantly enhanced IFN- $\beta$ -induced STAT1 nuclear translocation in ORF6-expressing cells [Figure 7B(10)–(12)]. In addition, Western blotting indicated NPIP3 C terminus overexpression enhancing IFN- $\beta$ -induced STAT1 phosphorylation at Tyr701 in ORF6-expressing cells (Figure 8). Results demonstrated that NPIP3 C terminus overexpression reduced Type I IFN

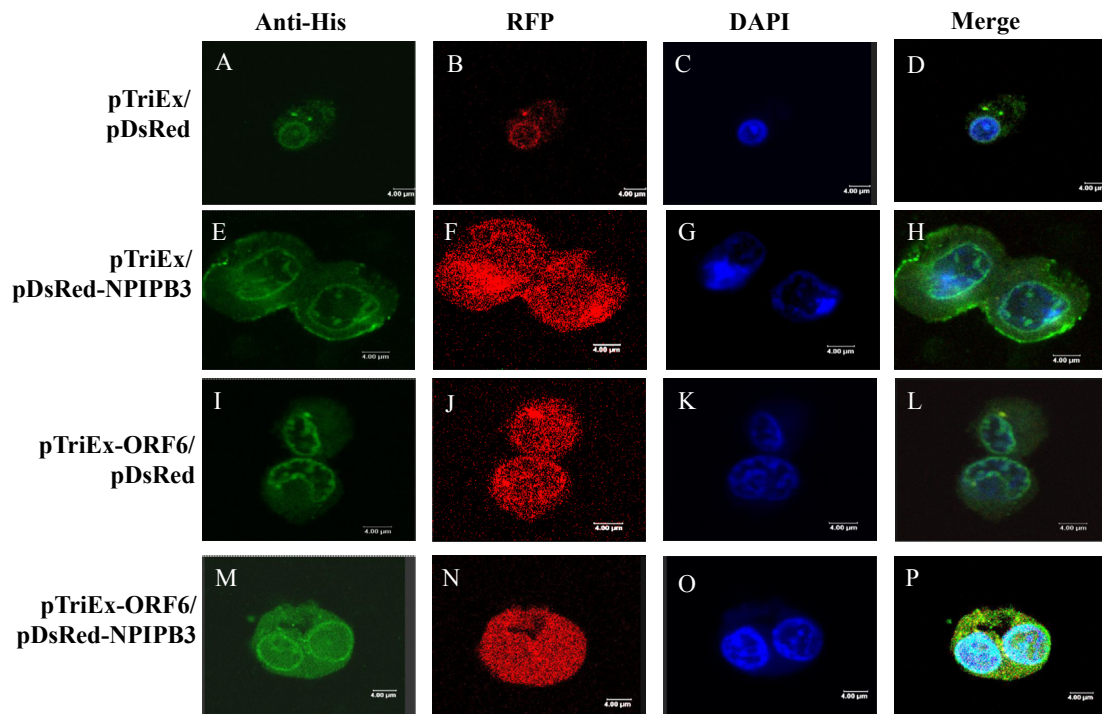


**Figure 5.** Colocalization analysis of SARS-CoV ORF6 and C-terminal domain of NPIP3 in human promonocytes using confocal microscopy. Transfected cells with single or both of pTriEx-ORF6 and pDsRed-NPIP3 were fixed, and stained with anti-His tag, followed by FITC-conjugated antimouse immunoglobulin G antibodies, and then analyzed by confocal microscopy. FITC = fluorescein isothiocyanate; NPIP3 = nuclear pore complex interacting protein family, member B3; ORF = open reading frame; SARS-CoV = severe acute respiratory syndrome coronavirus; Trx = thioredoxin.

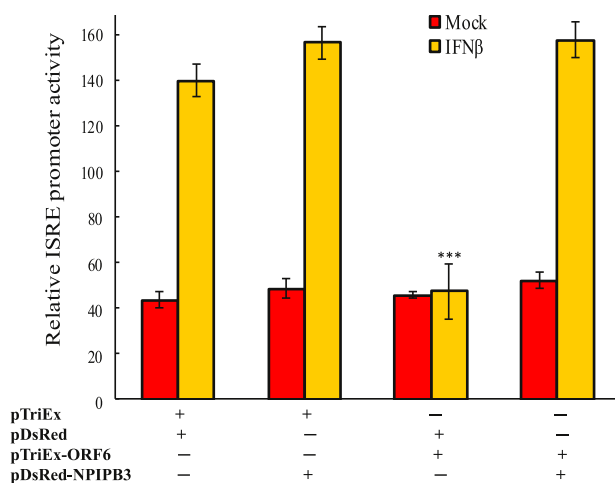


**Figure 6.** Effect of NPIP3 overexpression on the activity of the ISRE-based *cis* reporter. Cells were transiently cotransfected with single or both of pTriEx-ORF6 and pDsRed-NPIP3, plus control and ISRE luciferase reporters. Firefly and renilla luciferase enzymes were measured 4 hours after IFN- $\beta$  treatment. According to the dual Luciferase Reporter Assay System, the relative firefly luciferase activity was normalized by renilla luciferase. \*  $p < 0.05$ , by Scheffe's test. \*\*  $p < 0.01$ , by Scheffe's test. \*\*\*  $p < 0.001$ , by Scheffe's test. IFN = interferon; ISRE = IFN stimulated response element; NPIP3 = nuclear pore complex interacting protein family, member B3; ORF = open reading frame.

antagonism of SARS-CoV ORF6 via activating STAT1-mediated signal pathways.

## Discussion

The study demonstrated Type I IFN antagonism of SARS-CoV ORF6 through the inhibition of IFN- $\beta$ -induced STAT1 phosphorylation and nuclear translocation in human promonocytes (Figures 6–8), in agreement with a previous report in that ORF6 blocked STAT1 nuclear translocation in response to Type I IFNs via disrupting the import complex formation by binding with karyopherin alpha 2.<sup>6</sup> The C-terminal hydrophilic domain of ORF6 interacted with cellular karyopherins, but the N-terminal lipophilic part of ORF6 was also required for retaining cellular karyopherins at the ER/Golgi membrane, leading to impede nuclear import.<sup>15</sup> Besides STAT1, SARS-CoV ORF6 also affected the activity of karyopherin-dependent transcription factors, including VDR, CREB1, SMAD4, p53, Epas1, and Oct3/4.<sup>16</sup> Therefore, ORF6 plays the vital role in innate antiviral responses.

Biopanning of phage-displayed human lung cDNA libraries identified the binding interaction of ORF6 with its interacting host factors, including CCNL1, RBMXL2, and NPIP3 (Figures 2 and 3). CCNL1 displayed on phage clone number 16, containing an arginine- and serine-rich domain and a cyclin domain was required for spliceosome assembly and regulated splicing.<sup>17,18</sup> RBMXL2 displayed on phage clone number 26 was one of the heterogeneous nuclear

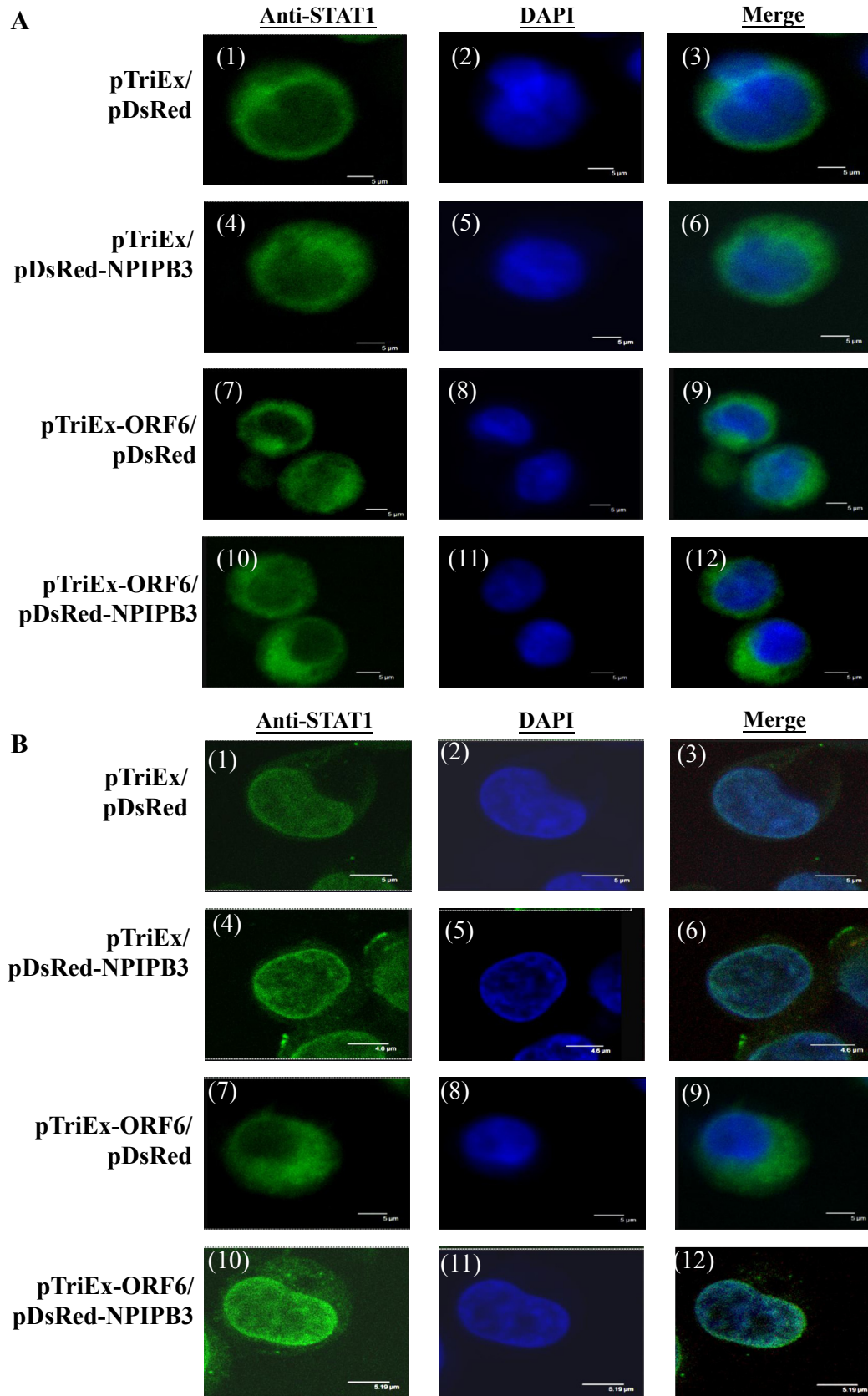


**Figure 7.** Effect of NPIP3 overexpression on IFN- $\beta$ -induced nuclear translocation of STAT1 in vector control and ORF6-expressing cells. (A) Mock and (B) IFN- $\beta$ -treated cells transfected with single or both of pTriEx-ORF6 and pDsRed-NPIP3 were fixed, and reacted with anti-STAT1 and FITC-conjugated antimouse immunoglobulin G antibodies. Finally, cells were stained with 4',6-diamidino-2-phenylindole (DAPI) for 10 minutes, imaging analyzed by confocal microscopy. FITC = fluorescein isothiocyanate; IFN = interferon; NPIP3 = nuclear pore complex interacting protein family, member B3; ORF = open reading frame; STAT1 = signal transducer and activator of transcription.



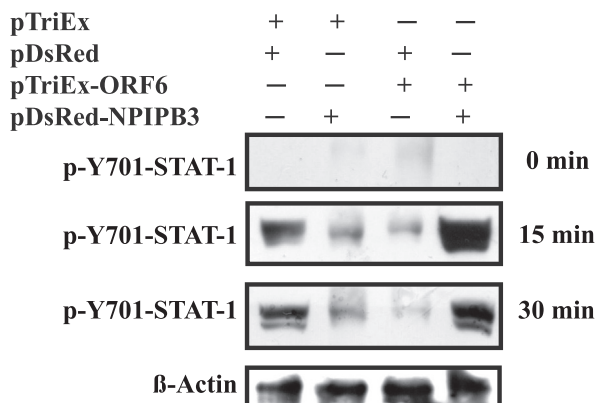


**Figure 8.** Effect of NPIP3 overexpression on IFN- $\beta$ -induced STAT1 phosphorylation at Tyr701 in vector control and ORF6-expressing cells using Western blotting. Cells were transiently transfected with single or both of pTriEx-ORF6 and pDsRed-NPIP3, and then treated with IFN- $\beta$ . After 0 minutes, 15 minutes, and 30 minutes of treatment, the lysate was analyzed by Western blotting with antiphosphotyrosine STAT1 (Tyr701), and anti- $\beta$ -actin antibodies. The immune complexes were visualized using horseradish peroxidase-conjugated goat antimouse immunoglobulin G antibodies and enhanced chemiluminescence. IFN = interferon; NPIP3 = nuclear pore complex interacting protein family, member B3; ORF = open reading frame; STAT1 = signal transducer and activator of transcription.

ribonucleoproteins, suggested as a germ cell-specific splicing regulator.<sup>19</sup> ORF6-interacting phage clone number 40 displayed the C-terminal domain of NPIP3 (Figures 2 and 3). NPIP3 had many *alternative names* such as nuclear pore complex-interacting protein-like 3, protein pps22-1, KIAA0220-like protein, nuclear pore complex-interacting protein B type, and PI-3-kinase-related kinase SMG-1 isoform 1 homolog.<sup>20</sup> NPIP3 containing a transmembrane region at the N terminus was recognized as a membrane protein and served as an RNA splicing factor. NPIP3 was upregulated in epithelial Caco-2 cells after exposure to probiotic *Lactobacillus acidophilus* L-92, linking with immune response, DNA binding, and protein synthesis.<sup>21</sup> NPIP3 was also identified to bind IFN- $\alpha$  promoter.<sup>22</sup> In this study, overexpression of NPIP3 C-terminal domain reduced the antagonistic activity of Type I IFN by SARS-CoV ORF6 protein (Figures 6–8). The diacidic cluster motif (residues 53–56) was found in the ORF6 protein, as the critical determinant of subcellular localization to vesicular structures.<sup>23</sup> Interestingly, the C-terminal domain of NPIP3 had several four positively charged residue (KRRR) repeats. Therefore, ionic interactions could be linked with the binding interaction between SARS-CoV ORF6 and NPIP3 C-terminal domain. In addition, the interaction between SARS-CoV ORF6 and NPIP3 C-terminal domain might influence the binding interaction between ORF6 and karyopherin alpha 2; thus, the C-terminal domain of NPIP3 recovered the nuclear import carrier function of karyopherin alpha 2 in ORF6-expressing cells, correlating with STAT1 nuclear translocation after IFN- $\beta$  treatment (Figure 7). In addition, overexpression of the NPIP3 C-terminal domain reduced IFN- $\beta$ -induced phosphorylation of

STAT1 at Tyr701 (Figure 8, lane 2). Tyrosine-protein kinase JAK1 (Janus kinase 1) contained a putative phosphoinositide binding site; an interaction between JAK1 and PI-3-kinase was reported in interleukin-2 signaling pathway.<sup>24</sup> Meanwhile, NPIP3, also known as PI-3-kinase-related kinase SMG-1, showed functional and structural similarities to PI-3-kinase.<sup>25</sup> Therefore, NPIP3 overexpression might increase the interaction with JAK1, which influenced IFN- $\beta$ -induced JAK/STAT signaling, resulting in the decrease of STAT1 phosphorylation at Tyr701.

In conclusion, SARS-CoV ORF6-interacting proteins including CCNL1, RBMXL2, NPIP3, and karyopherin alpha 2 were involved in RNA splicing, nuclear pore complex formation, as well as nuclear export and import of some transcription and splicing factors. This study demonstrated SARS-CoV ORF6 inhibiting IFN- $\beta$ -induced ISRE promoter, STAT1 nuclear translocation and phosphorylation. By contrast, the interaction of SARS-CoV ORF6 with the C-terminal domain of NPIP3 in human promonocytes reduced the Type I IFN antagonism of ORF6.

## Conflicts of interest

All authors have no conflicts of interest to declare.

## Acknowledgments

We would like to thank the Ministry of Science and Technology, Taiwan (MOST101-2320-B-039-036-MY3, and MOST102-2320-B-039-044-MY3) and China Medical University (CMU103-S-04, CMU101-ASIA-05, and CMU102-ASIA-15) for financial support.

## References

1. Drosten C, Günther S, Preiser W, van der Werf S, Brodt HR, Becker S, et al. Identification of a novel coronavirus in patients with severe acute respiratory syndrome. *N Engl J Med* 2003; **348**:1967–76.
2. Marra MA, Jones SJ, Astell CR, Holt RA, Brooks-Wilson A, Butterfield YS, et al. The Genome sequence of the SARS-associated coronavirus. *Science* 2003; **300**:1399–404.
3. Tan YJ, Lim SG, Hong W. Characterization of viral proteins encoded by the SARS-coronavirus genome. *Antiviral Res* 2005; **65**:69–78.
4. Narayanan K, Huang C, Makino S. SARS coronavirus accessory proteins. *Virus Res* 2008; **133**:113–21.
5. Liu DX, Fung TS, Chong KK, Shukla A, Hilgenfeld R. Accessory proteins of SARS-CoV and other coronaviruses. *Antiviral Res* 2014; **109**:97–109.
6. Frieman M, Yount B, Heise M, Kopecky-Bromberg SA, Palese P, Baric RS. SARS-CoV ORF6 antagonizes STAT1 function by sequestering nuclear import factors on the rER/Golgi membrane. *J Virol* 2007; **81**:9812–24.
7. Ye Z, Wong CK, Li P, Xie Y. A SARS-CoV protein, ORF-6, induces caspase-3 mediated, ER stress and JNK-dependent apoptosis. *Biochim Biophys Acta* 2008; **1780**:1383–7.
8. Yount B, Roberts RS, Sims AC, Deming D, Frieman MB, Sparks J, et al. Severe acute respiratory syndrome coronavirus group-specific open reading frames encode nonessential functions for replication in cell cultures and mice. *J Virol* 2005; **79**:14909–22.

9. Koepceky-Bromberg SA, Martinez-Sobrido L, Frieman M, Baric RA, Palese P. Severe acute respiratory syndrome coronavirus open reading frame (ORF) 3b, ORF 6, and nucleocapsid proteins function as interferon antagonists. *J Virol* 2007;**81**: 548–57.
10. Lin CW, Lin KH, Lyu PC, Chen WJ. Japanese encephalitis virus NS2B–NS3 protease binding to phage-displayed human brain proteins with the domain of trypsin inhibitor and basic region leucine zipper. *Virus Res* 2006;**116**:106–13.
11. Lin CW, Cheng CW, Yang TC, Li SW, Cheng MH, Wan L, et al. Interferon antagonist function of Japanese encephalitis virus NS4A and its interaction with DEAD-box RNA helicase DDX42. *Virus Res* 2008;**137**:49–55.
12. Lin YJ, Chang YC, Hsiao NW, Hsieh JL, Wang CY, Kung SH, et al. Fisetin and rutin as 3C protease inhibitors of enterovirus A71. *J Virol Methods* 2012;**182**:93–8.
13. Li SW, Lai CC, Ping JF, Tsai FJ, Wan L, Lin YJ, et al. Severe acute respiratory syndrome coronavirus papain-like protease suppressed alpha interferon-induced responses through downregulation of extracellular signal-regulated kinase 1-mediated signalling pathways. *J Gen Virol* 2011;**92**:1127–40.
14. Yang TC, Li SW, Lai CC, Lu KZ, Chiu MT, Hsieh TH, et al. Proteomic analysis for Type I interferon antagonism of Japanese encephalitis virus NS5 protein. *Proteomics* 2013;**13**:3442–56.
15. Hussain S, Gallagher T. SARS-coronavirus protein 6 conformations required to impede protein import into the nucleus. *Virus Res* 2010;**153**:299–304.
16. Sims AC, Tilton SC, Menachery VD, Gralinski LE, Schäfer A, Matzke MM, et al. Release of severe acute respiratory syndrome coronavirus nuclear import block enhances host transcription in human lung cells. *J Virol* 2013;**87**:3885–902.
17. Dickinson LA, Edgar AJ, Ehley J, Gottesfeld JM. Cyclin L is an RS domain protein involved in pre-mRNA splicing. *J Biol Chem* 2002;**277**:25465–73.
18. Graveley BR. Sorting out the complexity of SR protein functions. *RNA* 2000;**6**:1197–211.
19. Elliott DJ, Venables JP, Newton CS, Lawson D, Boyle S, Eperon IC, et al. An evolutionarily conserved germ cell-specific hnRNP is encoded by a retrotransposed gene. *Hum Mol Genet* 2000;**9**:2117–24.
20. Martin J, Han C, Gordon LA, Terry A, Prabhakar S, She X, et al. The sequence and analysis of duplication-rich human chromosome 16. *Nature* 2004;**432**:988–94.
21. Yanagihara S, Fukuda S, Ohno H, Yamamoto N. Exposure to probiotic *Lactobacillus acidophilus* L-92 modulates gene expression profiles of epithelial Caco-2 cells. *J Med Food* 2012;**15**:511–9.
22. Qu JH, Cheng J, Zhang LX, Zhong YW, Liu Y, Wang L, et al. Screening of binding proteins to interferon-alpha promoter DNA by phage display technique. *Zhonghua Gan Zang Bing Za Zhi* 2005;**13**:520–3.
23. Gunalan V, Mirazimi A, Tan YJ. A putative diacidic motif in the SARS-CoV ORF6 protein influences its subcellular localization and suppression of expression of co-transfected expression constructs. *BMC Res Notes* 2011;**4**:446.
24. Migone TS, Rodig S, Cacalano NA, Berg M, Schreiber RD, Leonard WJ. Functional cooperation of the interleukin-2 receptor beta chain and Jak1 in phosphatidylinositol 3-kinase recruitment and phosphorylation. *Mol Cell Biol* 1998;**18**: 6416–22.
25. Baretic D, Williams RL. PIKKs—the solenoid nest where partners and kinases meet. *Curr Opin Struct Biol* 2014;**29**:134–42.